Sensors and Materials, Vol. 35, No. 4 (2023) 1463–1472
MYU Tokyo

S & M 3260

Performance Analysis of Unmanned Aerial Vehicle Assisted Wireless IoT Sensors Based on Air-to-Ground Communication Model for Smart Farming

Sarun Duangsuwan[1*] and Sathaporn Promwong[2]

[1]Prince of Chumphon Campus, King Mongkut's Institute of Technology Ladkrabang,
17/1 Chumcoo District, Pathio, Chumphon 86160, Thailand
[2]School of Engineering, King Mongkut's Institute of Technology Ladkrabang,
1 Chalongkrung Rd., Ladkrabang, Bangkok 10520, Thailand

(Received October 16, 2022; accepted February 13, 2023)

Keywords: A2G communication, IoT sensors, UAV-assisted IoT, smart farming

We used an unmanned aerial vehicle (UAV) and IoT as a new platform for soil moisture monitoring based on the air-to-ground (A2G) communication model. We investigated an energy-efficient UAV trajectory by considering the power outage probability and transmission rate for UAV-assisted wireless IoT sensor connectivity. We considered the closed-form power outage probability for IoT sensors located within the coverage zone of a UAV drone small cell. We conducted experiments in the Napier and Ruzi grass farms with IoT sensors for detecting soil moisture along a drip line irrigation system located in the fields. The power outage probability is given for different UAV heights and transmission rates, which contributes to reliable communication with IoT sensors.

1. Introduction

Smart farming or precision agriculture is an innovative and integrated farming approach that enables the use of information and communication technologies (ICT) and innovative technologies such as unmanned aerial vehicles (UAVs) or drones,[1] IoT or wireless sensor networking,[2] robotics,[3] cloud computing or web applications,[4] artificial intelligence (AI)[5] and big data analytics[6] for effective decision-making.

Soil moisture monitoring is an essential application for smart farming to control plant growth and yield. Soil moisture is a key component of water irrigation and must be estimated.[7,8] Soil moisture monitoring using the IoT is a low-cost approach that rapidly collects data and can be applied to switch the water supply on and off via a mobile application.[9] Although IoT sensors were widely used in agricultural environments, the power signal constraint has limitations. Several pioneering studies have targeted UAV-assisted IoT sensor connectivity.[10–15]

Liu *et al.*[10] presented a method of resource allocation for UAV-assisted wireless IoT. The resources allocated by UAVs and the IoT are formulated using the dynamic game method to

*Corresponding author: e-mail: sarun.du@kmitl.ac.th
https://doi.org/10.18494/SAM4174

ISSN 0914-4935

control energy transfer and resource information between UAVs and the IoT. The schematics of the dynamic game method set the UAV as the leader and the IoT as the follower. The results of simulations showed that the dynamic game can apply multiple IoTs to almost 3500 devices within a processing time of 1 to 10 s. In Ref. 11, the authors proposed a measurement-aided dynamic planning algorithm (MAD-P) to optimize the position of a flying UAV to provide access to the backbone network for IoT devices. Then, the results of simulations using MAD-P of a drone small cell operating with multiple IoT sensors were introduced. The MAD-P is an asymptotic optimal method that can automatically solve the distributed fashion problem during drone flights. Huang *et al.*[12] then presented UAV-assisted simultaneous wireless information and power transfer (SWIPT). They discussed that some problems of infrastructure-starved IoT services involved the minimum energy harvested among the multiple ground sensors simultaneously transmitting data to the UAV. To solve this problem, they proposed an efficient iterative algorithm to jointly optimize the UAV transmit power allocation and trajectory. Likewise, joint UAV trajectory and resource allocation were presented in Ref. 13 for UAV-assisted powered IoT, for which results of simulations were obtained on the basis of asymptotic optimization. Thus, the UAV trajectory is essential for optimizing the power allocation to multiple IoT sensors. Na *et al.*[14] discussed that the optimized UAV trajectory can maximize the downlink achievable rate (bps/Hz) of all users for IoT deployment in emergency situations. Additionally, a schematic of artificial noise cancellation of an eavesdropper for UAV-assisted IoT was presented by Wang *et al.*[15] They discussed the effect of the probability of an eavesdropper based on a learning model.

In Refs. 10–15, the main contribution of UAV-assisted IoT connectivity was power allocation for an achievable rate of summation of IoT and UAV trajectories for power control or energy harvesting of multiple IoT connectivities. We applied a UAV as the drone small cell and IoT sensors to the agricultural model for the monitoring of soil moisture, as shown in Fig. 1. The

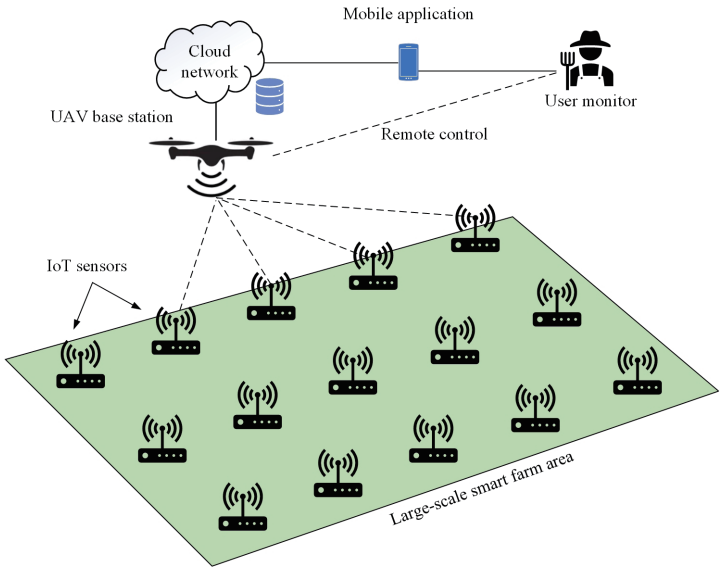

Fig. 1. (Color online) Soil moisture monitoring application using UAV and IoT sensors in a large-scale smart farm.

objective of this study was to investigate the identification of optimal trajectories for the UAV and evaluate the power outage probability versus the transmission rate between the UAV and IoT sensors. On the basis of a realistic propagation environment, we considered a new close-form derivation for UAV-assisted powered IoT sensing connectivity in such an application.

2. UAV-assisted Wireless IoT Connectivity

2.1 Air-to-ground (A2G) communication model

We considered a schematic of UAV-assisted wireless IoT sensing connectivity as illustrated in Fig. 2, where a UAV collects soil moisture data from IoT sensors within a coverage area of radius R. The UAV hovered over the center of the circular area at a height h_{UAV}. We assumed that k IoT sensors are randomly located within the UAV coverage area, and that the UAV and all IoT sensors were equipped with a single antenna.

The A2G communication systems were divided into two communication channels: the wireless power transfer or downlink h_k from the UAV to all IoT sensors, and the information transmission sink or uplink g_k, which involve data transmitted from the IoT sensors to the UAV or to the drone small cell, respectively. Additionally, we assumed that the IoT sensors do not have any prior power supply or charge in their built-in batteries for information transmission, while the UAV is equipped with two batteries. One UAV battery is used for flight, while the other is used for the wireless module.

The energy harvesting or the received signal strength at the IoT sensor depends on the Log-distance path loss, time of arrival τ_k, time of data collecting T, and UAV power transmitted P_0. The received signal strength indicator (RSSI) of the downlink channel is given by

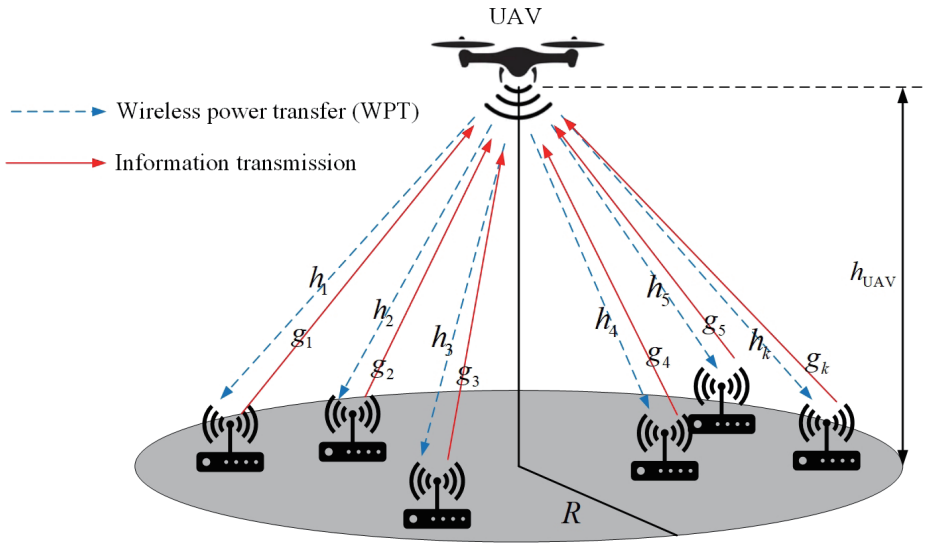

Fig. 2. (Color online) UAV-assisted wireless IoT sensing connectivity in the coverage area.

$$r_{do} = \left|h_k\right|^2 m_k P_0 \left(d, \tau_k\right) T. \tag{1}$$

The Log-distance path loss between the k sensors and UAV can be expressed as

$$m_k = \frac{\kappa}{d_k^{2n}}, \tag{2}$$

where d denotes the distance between the UAV and IoT sensor, n is the path loss exponent, and κ is the constant coefficient of the path loss. Herein, we assume that the distance between k IoT sensors and the UAV can be determined from the squared Euclidean distance as

$$\square^{\square} = {}_k + \square \quad , \tag{3}$$

where d_k represents the range between k IoT sensors and the center of the UAV coverage zone.

For the uplink channel, the energy consumption of information transmission from all IoT sensors to the UAV can be calculated as

$$r_{up} = \eta \frac{\tau_k}{1-\tau_k} \left|g_k\right|^2 m_k P_0 , \tag{4}$$

where η is the efficiency of energy harvesting for the IoT sensors.

In Eq. (4), a sufficient transmission rate of IoT sensors depends on the power consumption from the UAV P_0. Thus, the UAV trajectory and IoT location must be investigated. The signal-to-noise ratio (SNR) λ_k can be estimated by calculating the relationship between the uplink channel power $|g_k|^2$ and noise power N_0 in the additive white Gaussian noise (AWGN) channel as

$$\gamma_k = \left|h_k\right|^2 \left|g_k\right|^2 m_k \eta \frac{\tau}{1-\tau} \frac{P_0}{N_0} . \tag{5}$$

Thus, the achievable transmission rate (bps) for uplinking k IoT sensors can be written as

$$C_i = \left(1-\tau\right) \log_2 \left(1+\gamma_k\right). \tag{6}$$

2.2 Outage probability

From the A2G communication model, we consider the probability of a closed-form power outage versus the transmission rate for the uplink of IoT transmitted data to the UAV and cloud network. Then, the close-form outage probability can be written as

$$\begin{aligned}\Pr\left(C_i < R\right) &= \Pr\left(\frac{R}{1-\tau_k} > \log_2\left(1+\gamma_k\right)\right)\\ &= \Pr\left(\gamma_k < 2^{\frac{R}{1-\tau_k}} - 1\right)\\ &= \Pr\left(\frac{|h_k|^2 |g_k|^2}{\left(h_{\square}^2 + d_k^2\right)^n} \kappa\eta \frac{\tau_k}{1-\tau_k}\frac{P_0}{N_0} < \left(2^{\frac{R}{1-\tau_k}} - 1\right)\right)\\ &= \Pr\left(\frac{|h_k|^2 |g_k|^2}{\left(h_{\square}^2 + d_k^2\right)^n} \square \frac{\tau_k}{1-\tau_k}\frac{P_0}{N_0} < L\left(_k, R, \frac{P_0}{N_0}\right)\right),\end{aligned} \tag{7}$$

where $L\left(\tau_k, R, \frac{P_0}{N_0}\right) = \left(2^{\frac{R}{1-\tau_k}} - 1\right)\frac{1}{\kappa\eta}\frac{1-\tau_k}{\tau_k}\frac{N_0}{P_0}$. For a given d_k, the substitution (7) can be rewritten as

$$\Pr\left(C_i < R \middle| d_k\right) = \left(\left|h_k \cdot g_k\right| < \sqrt{L\left(\tau_k, R, P_0/N_0\right)\left(h_{\mathrm{UAV}}^2 + d_k^2\right)^n}\right). \tag{8}$$

3. Experimental Setup

The structure of a soil moisture kit is shown in Fig. 3(a). The components consist of a capacitive soil moisture sensor, an ESP8266 WiFi microcontroller, a voltage regulator, and a solar cell. The UAV base station is shown in Fig. 3(b); it is equipped with a wireless transmitter module under the body frame of the UAV body. The sensor frequency is based on a 2.4 GHz WiFi IEEE802.11g standard, the transmitter power is 100 mW or 20 dBm, and the flight time is 25 min.

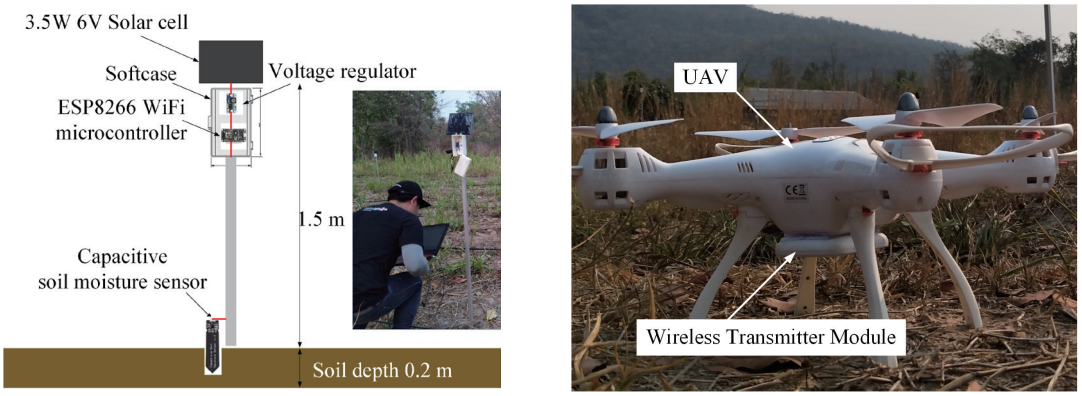

(a) (b)

Fig. 3. (Color online) (a) Soil moisture sensor kit and (b) UAV transmitter.

Figure 4(a) shows the layout of the soil moisture sensors along with the drip line irrigation in the Napier grass farm. The sensors are installed at a total of 12 positions, and NP11-NP34 represents the sensor positions. The dimensions of the Napier grass farm are a width of 25 m and a length of 45 m, as shown in Fig. 4(b). Figure 5(a) illustrates the layout of soil moisture sensors in the Ruzi grass farm, where the sensors are installed at 15 positions labeled RZ11 to RZ35. The dimensions of the Ruzi grass farm are a width of 30 m and a length of 50 m, as shown in Fig. 5(b).

Figure 6 shows the experimental test in the Napier and Ruzi grass farms. We consider the UAV trajectory at the center of the field, where the height of the vehicle started at 2 m and was

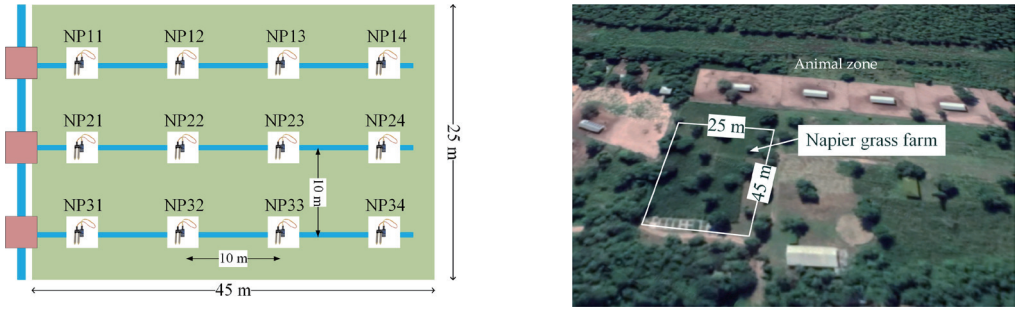

(a) (b)

Fig. 4. (Color online) (a) NP11 to NP34 positions and (b) dimension of the Napier grass farm in a satellite map.

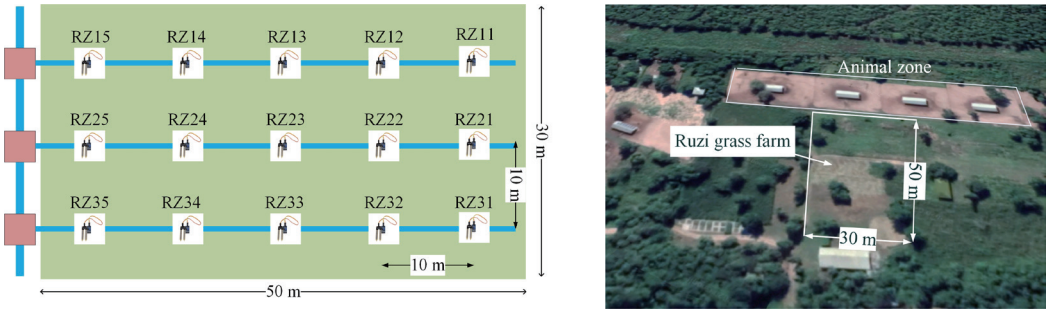

(a) (b)

Fig. 5. (Color online) (a) RZ11 to RZ35 positions and (b) dimension of the Ruzi grass farm in a satellite map.

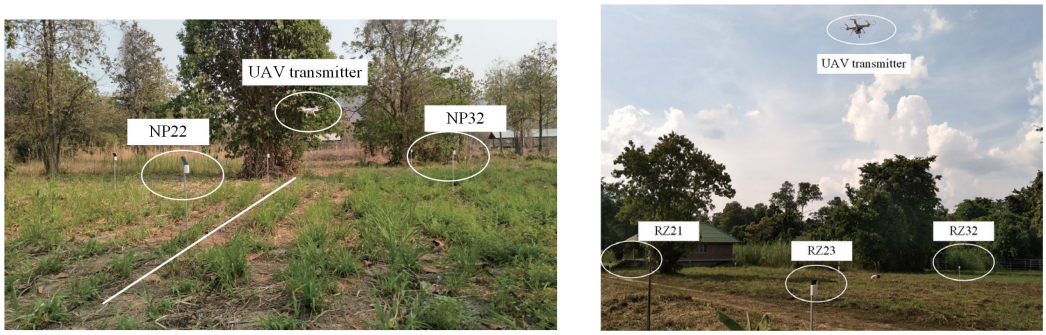

(a) (b)

Fig. 6. (Color online) Experimental test at (a) the Napier grass farm and (b) the Ruzi grass farm.

raised in 1 m increments until a height of 20 m was reached. The time of data collection per point was 1 min on average.

3.1 Network architecture

Figure 7 shows the capacitive soil moisture sensor that connects to the ESP8266 WiFi module with three lines from the analog interface, such as A0 signaling, GND, and 3.3V. The ESP8266 communicates with the wireless module on the UAV where the user interface (UI) device of each sensor is subscribed in the network server and authenticated in the message queuing telemetry transport (MQTT) broker/server. In the next step, the MQTT broker confirms the publication information to the application server when the user has already completed registration. We note that the network server is based on a cloud network or Google firebase platform, and the application server is a Grafana application server for the real-time monitoring of mobile applications by which the data are updated every 1 min. Table 1 shows the setup parameters. The mobile application shows the level of moisture percentage in the soil: a range of 1–45% is dry, 46–79% is humid, and 80–100% is wet.

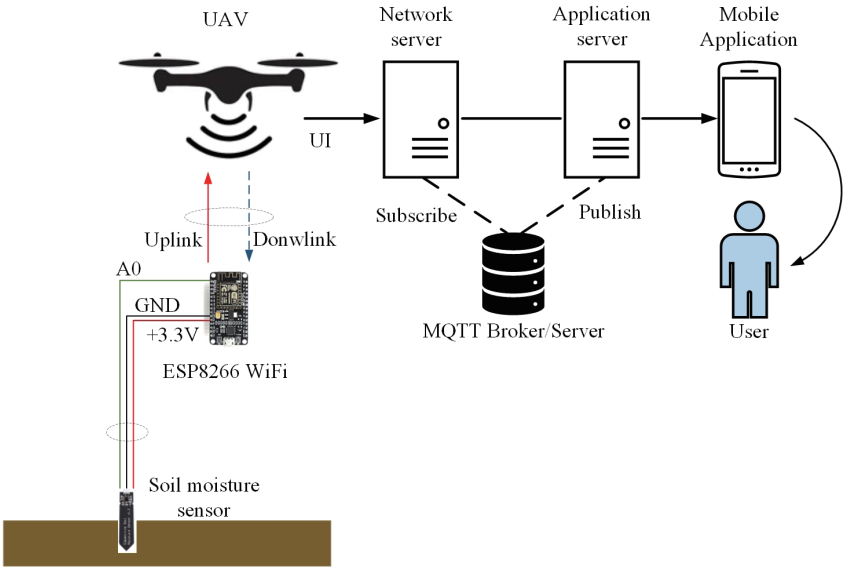

Fig. 7. (Color online) Network architecture.

Table 1
Experiment setup parameters.

Parameters	Value
UAV flight time	25 min.
Transmit power	20 dBm
Receiver sensitivity	−137 dBm
Modulation	FSK
Maximum bit rate	2 kbps
Payload length	4 bytes
Number of IoT sensors in Napeir grass farm	12 sensors
Number of IoT sensors in Ruzi grass farm	15 sensors

4. Results and Discussion

The results of the evaluation of power outage probability versus the UAV heights in the Napier and Ruzi grass farms are shown in Figs. 8 and 9, respectively. The power outage probability ranges from 0–1, which means that the power channel of the transmitter module at the UAV communicated with the IoT sensor on the ground. From the close-form formula in Eq. (8), the power outage probability depends on the UAV height and the distance to the IoT sensor $h^2_{\mathrm{UAV}} + d_k^2$. As a result, NP22 and NP23 are the positions with the highest power outage probability at 2 m until the UAV height reaches 20 m. The maximum power outage probability depends on the coverage area R of the UAV transmitter. While the minimum test points are NP34 and NP24, the effect of shadowing by trees attenuates the signaling to these sensors. The relative power outage probability results confirm that the communication link between the UAV and IoT sensor has a sufficient power channel $\left|h_k \cdot g_k\right|$ at a height of 20 m.

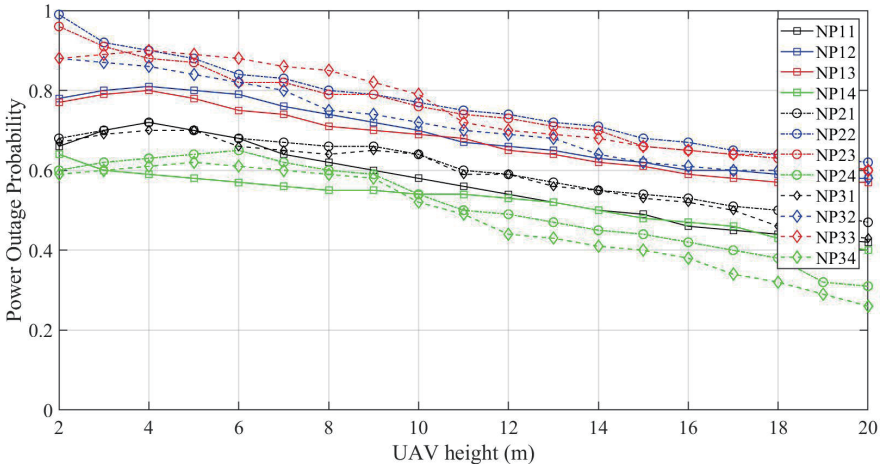

Fig. 8. (Color online) Power outage probability versus UAV height in the Napier grass farm test.

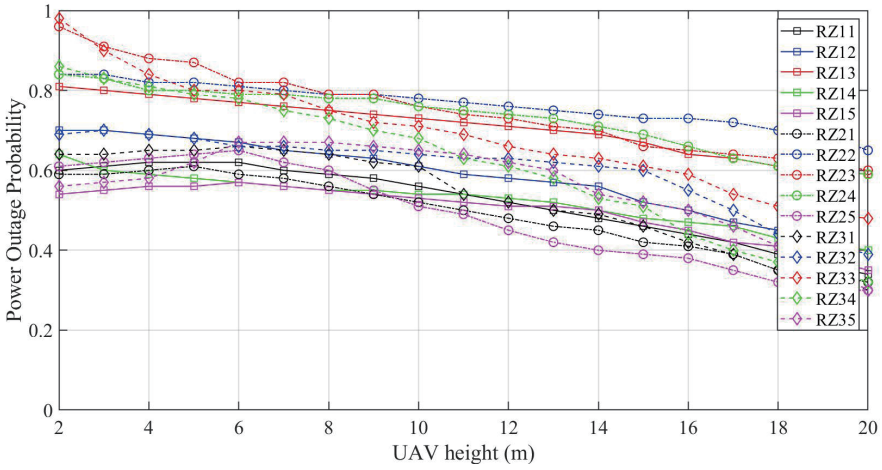

Fig. 9. (Color online) Power outage probability versus UAV height in the Ruzi grass farm test.

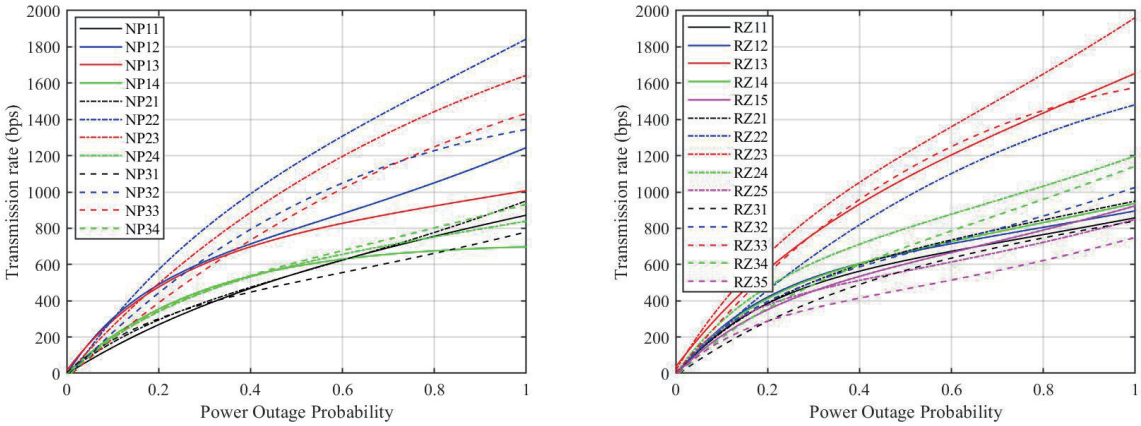

(a) (b)

Fig. 10. (Color online) Transmission rate versus the power outage probability between UAV and IoT sensors at the (a) Napier grass farm and (b) Ruzi grass farm.

After comparing the power outage probability with the UAV height, we evaluated the transmission rates versus the power outage probability, as shown in Fig. 10. The energy-efficiency of all IoT sensors depends on the power outage probability when the UAV moves along the height-defined trajectory. The transmission rates for all IoT sensors were monitored at the network server. The NP22 and RZ23 locations were the positions with the highest achievable transmission rate considering a power outage probability of 1 when the transmission rate guarantees almost the maximum rate.

5. Conclusions

We presented an analysis of the performance of UAV-assisted wireless IoT sensors for smart farming applications in the case of soil moisture monitoring. The objective of this study was to investigate the power channel and transmission rate in different scenarios such as those provided by the Napier and Ruzi grass farms. The determination of the closed-form power outage probability and transmission rates has been proposed as a means of investigating a reliable communication link between the UAV transmitter and all IoT sensors. The proposed method enabled us to investigate the energy efficiency of UAV-assisted wireless IoT sensors located in a realistic environment. In future work, path loss analysis and propagation delay will be considered.

References

1 M. Idbella, M. Iadaresta, G. Gagliarade, A. Mennella, S. Mazzoleni, and G. Bonanomi: Sensors **20** (2020) 1589. https://doi.org/10.3390/s20061589
2 N. G. S. Campos, A. R. Rocha, R. Gondim, T. L. Coelho da Silva, and D. G. Gomes: Sensors **20** (2020) 190. https://doi.org/10.3390/s20010190
3 A. Soheyb, T. Abdelmoutia, and T. S. Labib: Proc. 2021 4th Int. Symp. Advanced Electrical and Communication Technologies (ISAECT, 2021). https://doi.org/10.1109/ISAECT53699.2021.9668490

4 V. Moysiadis, K. Tsakos, P. Sarigiannidis, E. G. M. Petrakis, A. D. Boursianis, and S. K. Goudos: Proc. 2022 11th Int. Conf. Modern Circuits and Systems Technologies (MOCAST, 2022). https://doi.org/10.1109/MOCAST54814.2022.9837727
5 S. Qazi, B. A. Khawaja, and Q. U. Farooq: IEEE Access **10** (2022). https://doi.org/10.1109/ACCESS.2022.3152544
6 F. N. Fote, S. Mahmoudi, A. Roukh, and S. Ahme: Proc. 2020 5th Int. Conf. Cloud Computing and Artificial Intelligence: Technologies and Applications (CloudTech, 2020). https://doi.org/10.1109/CloudTech49835.2020.9365869
7 K. Priandana, and R. AI-Fatihah Wahyu: Proc. 2020 Int. Conf. Smart Technology and Applications (ICoSTA, 2020). https://doi.org/10.1109/ICoSTA48221.2020.1570615896
8 J. A. T. Urmeneta and J. R. N. de Ios Santos: Proc. 2020 IEEE 12th Int. Conf. Humanoid, Nanotechnology, Information Technology, Communication and Control, Environment, and Management (HNICEM, 2020). https://doi.org/10.1109/HNICEM51456.2020.9400019
9 S. Duangsuwan, C. Teekapakvisit, and M. M. Maw: Adv. Sci., Tech. Eng. Syst. J. **5** (2020) 4. https://dx.doi.org/10.25046/aj0504244
10 B. Liu, H. Xu, and X. Zhou: Sensors **19** (2019) 1908. https://doi.org/10.3390/s19081908
11 N. Li, Y. Zhou, C. Shi, N. Cheng, L. Cai, and B. Li: IEEE Internet of Things J. **6** (2019) 2. https://doi.org/10.1109/JIOT.2018.2873772
12 F. Huang, J. Chen, H. Wang, and G. Ding: IEEE Access **7** (2019) 68260. https://doi.org/10.1109/ACCESS.2019.2918135
13 Z. Na, M. Zhang, J. Wang, and Z. Gao: Ad Hoc Net. **98** (2020) 102052. https://doi.org/10.1016/j.adhoc.2019.102052
14 Z. Na, B. Mao, J. Shi, J. Wang, Z. Gao, and M. Xiong: Physi. Commun. **41** (2020) 101100. https://doi.org/10.1016/j.phycom.2020.101100
15 Q. Wang, H-N. Dai, X. Li, M. K. Shukla, and M. Imran: Comput. Commun. **164** (2020) 1. https://doi.org/10.1016/j.comcom.2020.09.017

About the Authors

Sarun Duangsuwan received his B.Eng. and M.Eng. degrees in Information Engineering and his D.Eng. degree in Electrical Engineering from King Mongkut's Institute of Technology Ladkrabang, Thailand, in 2008, 2010, and 2015, respectively. Since 2018, he has been an assistant professor at King Mongkut's Institute of Technology Ladkrabang, Prince of Chumphon Campus. His research interests are in IoT sensors, UAV-enabled wireless communication, and their application to smart agriculture. (sarun.du@kmitl.ac.th)

Sathaporn Promwong received his B.Ind. degree in Electronics and M.Eng. degree in Electrical Engineering from King Mongkut's Institute of Technology Ladkrabang, Thailand, in 1994 and 1996, respectively, and his Ph.D. degree in Communications and Integrated Systems from Tokyo Institute of Technology, Japan, in 2008. Since 2018, he has been an assistant professor at King Mongkut's Institute of Technology Ladkrabang. His research interests are in wireless communications and wireless sensor networks. (sathaporn.pr@kmitl.ac.th)